Spectroscopy Of Light Lead And Actinide Nuclei Using An Evaporation Residue Detector

W. Reviol, D.G. Sarantites, R.J. Charity, C.J. Chiara, J. Elson, M. Montero, O.L. Pechenaya, S.K. Ryu, and L.G. Sobotka

Chemistry Department, Washington University, St. Louis, MO 63130, USA

Abstract. A high-efficiency evaporation-residue counter (named HERCULES) has been built. It consists of 64 thin fast-plastic scintillators arranged in four angular rings. Its design has been optimized for use with GAMMASPHERE. Presented are: the design and performance of the detection system, the most important results from its commissioning run (using ^{48}Ti + ^{126}Te and ^{48}Ti + ^{142}Nd reactions), and a brief outlook for spectroscopic studies in the actinide region.

INTRODUCTION

The spectroscopy of light lead and actinide nuclei produced in fusion-evaporation reactions is hampered by the presence of a large fission background. In particular, the in-beam spectroscopy of these species, at medium and high spin, requires a filter or "tag" to separate the γ rays of the evaporation residues from those of the fission products and other sources of background. There are several solutions to this problem: (1) Recoil mass separation and recoil decay tagging, using a mass separator such as the FMA device and associated detector equipment (see e.g. Ref. [1]). (2) Detection of the evaporation residues by time-of-flight and pulse height with a dedicated detection system (see e.g. Ref. [2]). (3) Isomer tagging at the target position (see e.g. Ref. [3]). These are rather complementary methods. For example, in a FMA experiment nearly symmetric reactions and a thin target are required (due to the small angular acceptance of the device), whereas a residue detector is most efficient when an asymmetric reaction and a ~ 1 mg/cm^2 thick target (that causes much straggling) is used. For the same reason, access to αxn evaporation channels is often excluded in a mass separator experiment (since these residues receive a large "side-kick") but is easy to achieve with a residue detector. Notice that αxn channels are important in the production of very heavy nuclei (see e.g. Ref. [4]).

Prior to this work, evaporation-residue detectors have been used in several spectroscopic and reaction studies. Ward *et al.* utilized the secondary electrons produced by evaporation-residue products when traversing a foil as a tag to perform spectroscopy in the presence of an intense fission background [5]. Heese *et al.* refined this concept in the design of an 18-element Recoil Filtering Device (RFD) [2]. At the front end of each RFD element, secondary electrons are produced when recoiling ions hit a Mylar foil. These electrons are accelerated and focussed on plastic scintillator foils. The cylindrical RFD elements cover (in part) forward angles between 2° and 15°. The RFD is compact and thus easy to combine with any Ge γ-ray detector array, e.g. with the full size GAMMASPHERE [6]. For a reaction study (of a rather light system), Ajitanand *et al.* chose to detect the evaporation residues directly with a thin fast-plastic detector [7].

We have designed and built a different system of evaporation-residue detectors and have named it HERCULES ($\mathscr{H}$igh $\mathscr{E}$fficiency $\mathscr{R}$esidue $\mathscr{C}$ounter $\mathscr{U}$nder $\mathscr{L}$ots of $\mathscr{E}$lastic $\mathscr{S}$cattering). The basic method of residue detection is the same as in Ref. [7]. However, the construction of the HERCULES array and custom electronics, and our new insights in the light-output characteristics and radiation hardness of thin plastic scintillators for heavy ions, has turned this technique into a high efficiency method suitable for use with GAMMASPHERE. Due to its large solid-angle coverage, high granularity, and fast timing, the efficiency of HERCULES equals and probably surpasses that of the RFD. It is anticipated that HERCULES will be mainly used to facilitate γ-ray spectroscopic studies in the trans-lead region.

CP764, *Nuclei at the Limits,* edited by D. Seweryniak and T. L. Khoo

DETECTOR DESIGN

The HERCULES device separates the evaporation-residue products from fission fragments and other reaction debris by time-of-flight and pulse-height analysis. The following design requirements are met:

1. High segmentation to reduce the counting rate in each detector element.
2. Sufficiently thin fast-plastic scintillators to stop only the heavy evaporation residues and allow the lighter species to go through.
3. Response to high-Z evaporation-residue products with good efficiency and with pulse heights well above noise.
4. Radiation damage: the scintillators "survive" for several days in a bombardment with elastically-scattered beam particles.
5. Fast electronics: full signal recovery in ~ 10 ns to avoid the pileup that can occur between an evaporation residue and elastic scattering.
6. Geometry: all residues reach the detectors before the elastically-scattered beam from the next beam burst.

The design involves an array of 64 plastic scintillators (~ 1 mg/cm^2 thick) coupled via arc-shaped light guides to photomultiplier tubes. The detectors are arranged in four rings as indicated in Table 1. The detector array can be positioned at any distance between 22.6 and 40.0 cm from the target. To achieve access to 19.1 °, the first ring of GAMMASPHERE is removed – i.e. HERCULES is compatible with 103 Ge detectors.

TABLE 1. Number of detectors and subtended angles of the HERCULES array. The angles correspond to a distance of the array of 30.9 cm from the target. The average angles listed in the last column are for later reference.

Ring	Detectors	θ°_{in}, θ°_{out}	msr/det.	msr/ring	θ°_{avg}
1	8	3.2, 7.1	5.16	41.3	5.15
2	14	7.2, 11.2	5.27	73.8	9.2
3	18	11.3, 15.2	5.70	102.6	13.25
4	24	15.3, 19.1	5.35	128.4	17.20

The detector characteristics have been established in both in-beam test experiments (at the ATLAS accelerator) and extensive source experiments with a ^{252}Cf source. Perhaps most crucial is the third point listed above; a brief discussion of this follows (for more details see Ref. [8]).

In order to study the Z dependence of the scintillator pulse height we carried out source measurements with an energy-degraded ^{252}Cf source (using Al foils of various thicknesses in front of the source). The groups of the light and heavy fission fragments have average Z values of 42 and 56, respectively. It is found that, for fragments stopped in a scintillator, the differentiation in pulse height with Z disappears in the energy range between about 8 and 45 MeV and only the energy dependence of the pulse height remains. This is consistent with a reduction in light-output quenching. Notice that the range for the absorbed energy $E \lesssim 45$ MeV represents a region well below the Bragg peak (maximum value of the electronic stopping power as a function of the incident energy of the ion). Furthermore, it can be shown that in this energy region the light output per unit energy increases with decreasing energy [8]. While a substantial pulse height is measured down to 8 MeV, the light production must approach a zero value for $E \to 0$ (not covered by our measurements).

The substantial pulse height of very low-energy residues is a result of the reduction in quenching at the low absorbed energies and the fact that dE/dx for heavy ions with energies $\gtrsim 5$ MeV, even for very heavy nuclei, is dominated by electronic energy loss [9]. These are the reasons why HERCULES works as a residue counter for very heavy nuclei.

IN-BEAM PERFORMANCE

In the commissioning run of HERCULES, a series of experiments was carried out using ^{48}Ti + ^{126}Te and ^{48}Ti + ^{142}Nd reactions. The former reaction was performed utilizing two different beam intensities, while in the latter case the beam energy and the target thickness were varied. In the ^{48}Ti + ^{142}Nd case, a 230-MeV beam was focussed on a 0.46 mg/cm^2 ^{142}Nd foil with 0.05 and 0.37 mg/cm^2 gold on the front and the back, respectively (A), as well as on a 1.10 mg/cm^2 target foil between 0.16 (front) and 0.48 mg/cm^2 gold (back) (B). A 238-MeV beam impinged on the same

0.46 mg/cm^2 ^{142}Nd target (C) and a target stack with a total of 1.04 mg/cm^2 ^{142}Nd and 0.27, 0.10, and 0.37 mg/cm^2 gold at the front, the center, and the back of the stack, respectively (D).

The experiment was performed at the 88" Cyclotron at the Lawrence Berkeley National Laboratory. The GAMMASPHERE array was comprised of 102 Compton-suppressed Ge detectors. The event trigger required a minimum of four Compton-suppressed Ge detectors firing in prompt coincidence. The information from any of the HERCULES detectors that was correlated with the event trigger was accepted as well. As indicated in Table 1, a distance of 30.9 cm between the HERCULES detectors and the target was chosen. However, ring 1 was partially shielded so that HERCULES covered angles from 5.6° to 19.1° (ring 1: $\theta_{avg} = 6.35°$).

The evaporation-residue identification is best accomplished with two-dimensional maps of time-of-flight vs. scintillator pulse height. The very high singles counting rate of the elastic scattering in each HERCULES detector are expected to create copious amounts of random events that appear about 10 ns after each beam burst.

In Fig. 1, time-of-flight vs. pulse height maps from the ^{48}Ti + ^{142}Nd reaction are shown. For this plot, representative detectors in each ring have been chosen. The evaporation-residue events (ER) are seen between the first two beam bursts as a group with low pulse heights. The debris from competing reactions are seen as excessive counts near the beam burst preceding the evaporation residues. These reactions include fission products, elastically-scattered beam particles off the ^{142}Nd target and the ^{197}Au backing, elastically-scattered target recoils, and ^{197}Au recoils, and fusion products due to oxidation of and carbon deposits on the target. The residue cross section is on the order of 1 mb, while the Bass fusion cross section is 180 mb. Notably, the residue group has no significant contamination from the debris. This observation is supported by the example of a spectroscopic measurement in the lead region shown in Fig. 2.

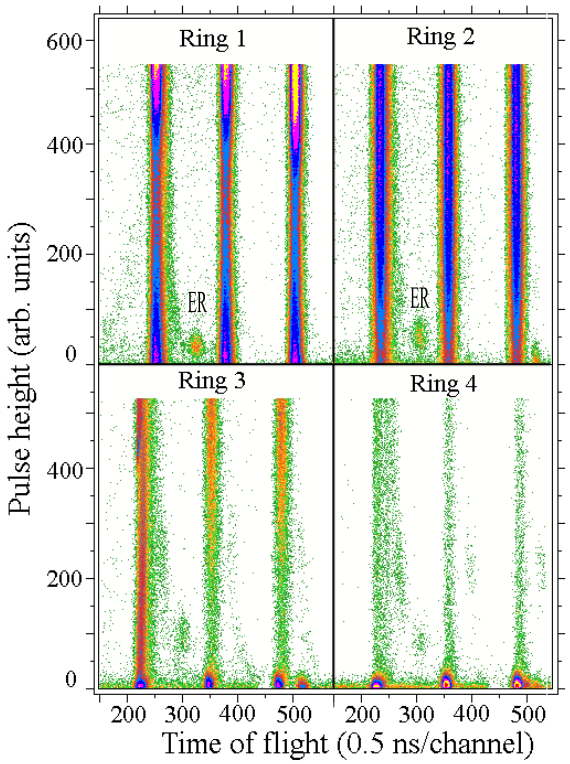

FIGURE 1. Time-of-flight vs. pulse height for one detector from each ring of *hercules*. The data are from the 230-MeV ^{48}Ti + ^{142}Nd reaction (with the 0.46 mg/cm^2 target foil) at a beam intensity of 1.5 pnA. Notice that the beam period is 67 ns and that the maximum pulse height of the elastic events is off scale.

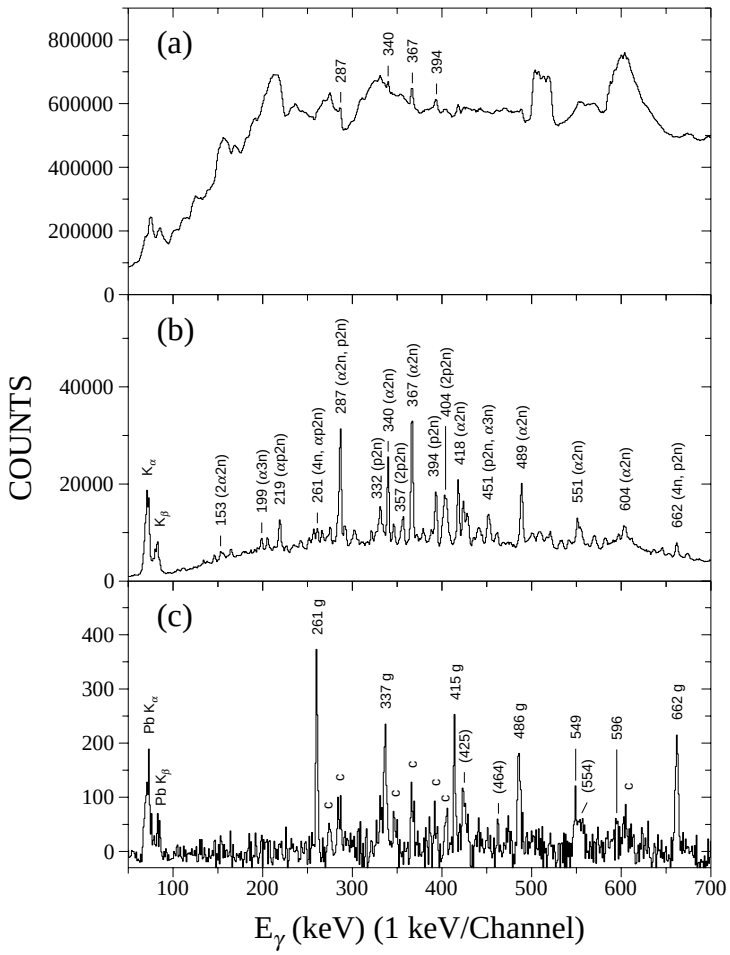

FIGURE 2. (a) A "raw" γ-ray spectrum from the ^{48}Ti + ^{142}Nd reaction. (b) The spectrum gated by residues (and requiring certain γ-ray fold conditions). The prominent γ rays in the respective exit channels are identified as well as the composite X-ray peaks. (c) A representative spectrum for ^{186}Pb obtained from data gated as in (b) and a sum of γ-ray double gates. The gating transitions are marked by g, known transitions from contaminant nuclei by c.

The spectrum of Fig. 2(a) is the sum spectrum for the conditions (A), (B), and (D) where only a Doppler-shift correction is applied. A peak-to-background ratio ~ 0.05 is observed. The corresponding spectrum after gating on evaporation-residue events (and on a different γ-ray fold for (A), (B), and (D) [10]) is shown in panel (b). As a result of the residue gating, the peak-to-background ratio is ~ 3.1 for the strongest transitions; this represents an improvement by one and a half orders of magnitude.

The goal of this analysis was to obtain new spectroscopic information for ^{186}Pb + 4n (and the purpose of the fold gating was to enhance the known [2, 11] transitions in ^{186}Pb). However, the spectrum of Fig. 2(b) is dominated by other evaporation channels, in particular ^{184}Hg + α2n and ^{187}Tl + p2n. By carefully gating on prominent γ rays of ^{186}Pb it is possible to proceed. Figure 2(c) shows the yrast sequence obtained from a double-gating procedure. The strongest γ rays in this sequence could be established as electric quadrupole ($E2$) transitions from an angular-distribution analysis [10]. However, the ^{48}Ti + ^{142}Nd reaction is not the optimum choice to study ^{186}Pb + 4n with the present setup (angle coverage $\geq 5.6°$). Instead the ^{36}Ar + ^{154}Gd reaction (like in Refs. [2, 11]) or an even more asymmetric reaction would be favorable.

The efficiency for HERCULES is determined from the intensity ratio for a prominent peak in a residue-gated and a "raw" γ-ray spectrum and depends on the conditions for the reaction as well as on the reaction channel. In the commissioning run, three major effects have been observed:

1. Decrease in efficiency as a function of the counting rate (observed for different beam intensities).
2. Increase in efficiency for αxn channels compared to pxn or xn channels (related to angular distribution).
3. Increase in efficiency with target thickness (related to straggling).

Representative efficiency values measured for the 230-MeV ^{48}Ti + ^{142}Nd reaction and the thicker target (B) are 19.5(7)% for the α2n channel and 13.2(6)% for the p2n channel. The corresponding values for the thinner target (A) are 14.2(7)% (α2n) and 10.2(5)% (p2n). Notice that efficiency values for an xn channel could be only obtained from the ^{48}Ti + ^{126}Te data. Since the residue angular distributions for xn and pxn channels are similar, one may expect that the corresponding efficiencies are similar too.

The residue angular distributions for certain reaction channels are determined by comparing the γ-ray spectra separately gated by the HERCULES detectors in each ring. To compare these distributions for both different reaction channels and target thicknesses, the data are normalized to the respective values for ring 2. Prior to normalization the data are corrected for pileup losses; these are at most 20% (ring 1, thicker target). The resulting angular distributions for the 230-MeV ^{48}Ti + ^{142}Nd reaction are shown in Figs. 3(a) and (b).

Simulations of residue angular distributions have been performed, examples of which are shown in Fig. 3(c). The relevant distributions $d\sigma/d\theta(\theta)$ in this plot are those where the lateral straggling of the residue events in the target material [9] is taken into account (thick lines). Notice that Fig. 3(c) represents the "worst" case (smallest amount of straggling). For the comparison with the data in Figs. 3(a) and (b), the calculated differential cross section is integrated over a certain angular range (the range covered by a certain detector ring) and normalized to the value obtained for the range covered by ring 2. Overall, the simulations reproduce the experimental angular distributions. It should be pointed out that, at the ring 1 position, the normalized cross section for the p2n channel is calculated to be always larger than that for the α2n channel. This is consistent with the experimental observations and indicates that ring 1 covers the maximum of the residue angular distribution for the α2n channel, or is at least close to it (depending on the target thickness), but does not cover the maximum for the p2n channel. Hence, the detection efficiency is larger for the α2n products than for the p2n products.

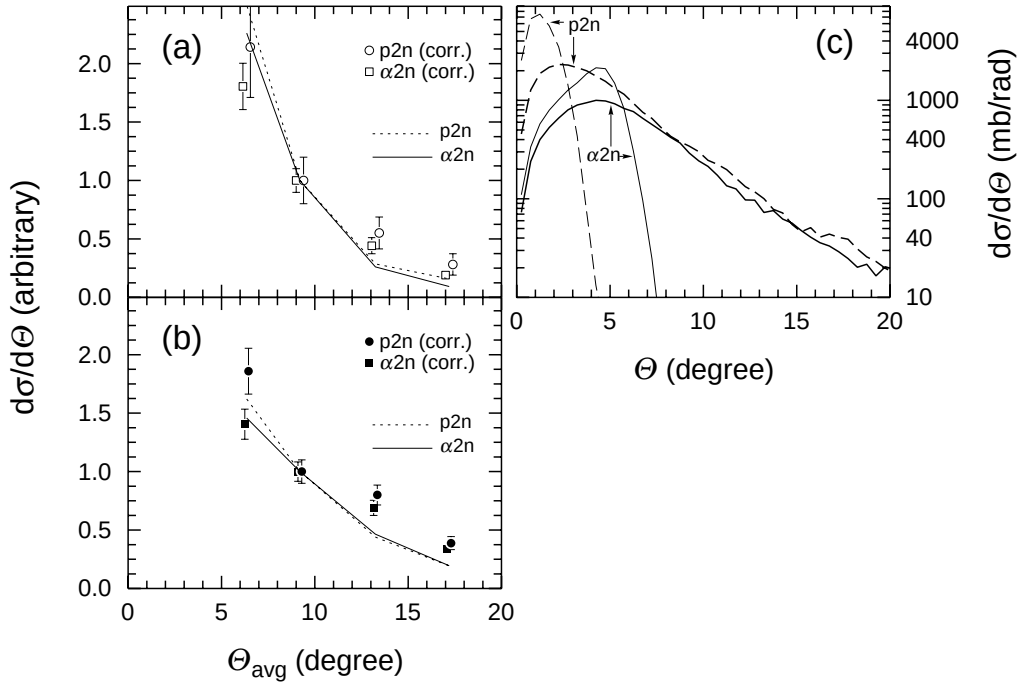

FIGURE 3. The pileup-corrected, normalized residue angular distributions for the 230-MeV ^{48}Ti + ^{142}Nd reaction compared with results from simulations. The simulated four-point angular distributions are connected to each other by lines. Panels (a) and (b) represent the cases for a target with 0.46 mg/cm^2 ^{142}Nd and 1.10 mg/cm ^{2} ^{142}Nd, respectively. Panel (c) is the calculated differential cross section as a function of lab angle for prominent evaporation channels and no fission in this reaction. The thin dashed and solid lines are for the p2n and α2n channels, respectively. The corresponding thick lines show the angular distributions when straggling in the target (0.46 mg/cm^2 plus gold) is included.

CONCLUSION AND OUTLOOK

A 64-element fast-plastic evaporation-residue detector named HERCULES has been designed and constructed. The device design has been optimized for use with GAMMASPHERE. Evaporation residues are well separated from elastic scattering, fission products, and other undesired reaction debris by time-of-flight (within one beam period) and pulse height. The commissioning run of HERCULES provided a proof-of-principle and produced first spectroscopy results for the very fissile system ^{48}Ti + ^{142}Nd $\rightarrow$ ^{190}Pb* (particularly, γ-ray angular distributions for yrast transitions in ^{186}Pb were measured).

The detection efficiency for evaporation residues is high. For the ^{48}Ti + ^{142}Nd reaction in the commissioning run, efficiencies of $\sim$ 20% (α2n) and $\sim$ 15% (p2n) are measured, at a beam intensity of 1.5 pnA. A rate-dependent reduction of the efficiencies has been observed (and is mainly attributed to a non-optimum electronics setup in the commissioning run [8]). The efficiency has to be maximized by appropriate choices of the beam-target combination (residue angular distribution) and the target thickness (straggling). Very asymmetric reactions (using beams considerably lighter than ^{48}Ti) and monolayer targets with surface densities $\gtrsim 0.5$ mg/cm^2 are favorable.

The anticipated main application of the HERCULES device is to facilitate detailed γ-ray spectroscopy of trans-lead nuclei using fusion-evaporation reactions. Such experiments would benefit from this device in two respects: (1) Both xn and αxn reaction channels can be simultaneously studied in one experiment. (2) There is the option to use rather light beams (perhaps as light as neon) which probably lead to higher residue cross sections than those obtained in symmetric reactions. The first point is an important asset. The αxn channel is the dominant evaporation channel for many compound systems in the actinide region, particularly as one goes from, say, Z = 89 (actinium) towards higher Z (see discussion in Ref. [4]) or/and as one goes towards lighter systems within an isotopic chain (see cross-section measurements of Ref. [12]).

ACKNOWLEDGMENTS

The assistance and advice of colleagues from Argonne (R.V.F. Janssens, C.J. Lister, D. Seweryniak, J. Greene), Berkeley (P. Fallon, A.O. Macchiavelli, M. Cromaz), and HMI-Berlin (K.H. Maier) in the course of this work is acknowledged. This work was supported by US DOE under grant no. DE-FG02-88ER-40406.

REFERENCES

1. M. P. Carpenter *et al.*, Phys. Rev. Lett. **70**, 3650 (1997); and references therein.
2. J. Heese, K. H. Maier, H. Grawe, J. Grebosz, H. Kluge, W. Meczynski, M. Schramm, R. Schubart, K. Spohr, and J. Styczen, Phys. Lett. **B302**, 390 (1993); and references therein.
3. G. D. Dracoulis, G. J. Lane, A. P. Byrne, A. M. Baxter, T. Kibedi, A. O. Macchiavelli, P. Fallon, and R. M. Clark, Phys. Rev. C **67**, 051301(R) (2003).
4. P. T. Greenlees *et al.*, J. Phys. G **24**, L63 (1998).
5. D. Ward, G. D. Dracoulis, J. R. Leigh, R. J. Charity, D. J. Hinde, and J. O. Newton, Nucl. Phys. **A406**, 591 (1983).
6. I. Y. Lee, Nucl. Phys. **A520**, 641c (1990).
7. N. N. Ajitanand, M. Beuhler, C. Gelderloos, and J. M. Alexander, Nucl. Instrum. Methods **A316**, 446 (1992).
8. W. Reviol, D. G. Sarantites, R. J. Charity, C. J. Chiara, J. Elson, M. Montero, O. L. Pechenaya, S. K. Ryu, and L. G. Sobotka, Nucl. Instrum. Methods **A** (submitted).
9. J. F. Ziegler, http://www.srim.org.
10. W. Reviol, C. J. Chiara, O. Pechenaya, D. G. Sarantites, P Fallon, and A. O. Macchiavelli, Phys. Rev. C **68**, 054317 (2003).
11. A. M. Baxter *et al.*, Phys. Rev. C **48**, R2140 (1993).
12. C.-C. Sahm, H.-G. Clerc, K.-H. Schmidt, W. Reisdorf, P. Armbruster, F. P. Hessberger, J. G. Keller, G. Munzenberg, and D. Vermeulen, Nucl. Phys. **A441**, 316 (1985).